



HAL
open science

On granular rheology in bedload transport

Raphael Maurin, Julien Chauchat, Bruno Chareyre, Philippe Frey

► **To cite this version:**

Raphael Maurin, Julien Chauchat, Bruno Chareyre, Philippe Frey. On granular rheology in bedload transport. CFM 2015 - 22ème Congrès Français de Mécanique, Aug 2015, Lyon, France. hal-03444975

HAL Id: hal-03444975

<https://hal.science/hal-03444975>

Submitted on 23 Nov 2021

HAL is a multi-disciplinary open access archive for the deposit and dissemination of scientific research documents, whether they are published or not. The documents may come from teaching and research institutions in France or abroad, or from public or private research centers.

L'archive ouverte pluridisciplinaire **HAL**, est destinée au dépôt et à la diffusion de documents scientifiques de niveau recherche, publiés ou non, émanant des établissements d'enseignement et de recherche français ou étrangers, des laboratoires publics ou privés.

On granular rheology in bedload transport

R. Maurin^a, J. Chauchat^b, B. Chareyre^c and P. Frey

a. Irstea, Grenoble, UR ETGR, Univ. Grenoble Alpes. raphael.maurin@irstea.fr

b. LEGI, CNRS UMR 5519, Univ. Grenoble Alpes.

c. 3SR, CNRS UMR 5521, Univ. Grenoble Alpes.

Abstract :

The local granular phase rheology in bedload transport is investigated from discrete numerical simulations. The numerical model is based on a coupled Discrete Element Method with a 1D space-averaged fluid momentum balance. Using this model the averaged granular stress tensor profile can be computed from particle-particle interactions. In bed-load transport, the granular media exhibits quasi-static and dynamical behaviors. This physical situation can be used as a rheometer and the actual granular rheology can be deduced from a single simulation. Preliminary results suggests that the denser part of the flow, close to the static bed, is well described by a $\mu(I)/\phi(I)$ rheology. Above this layer, the dense granular flow rheology fails to explain the observed shear and normal stresses, meaning that other mechanisms come into play.

Key words: granular rheology, bedload, DEM.

1 Introduction

In sediment transport, bedload is characterized by particles rolling, sliding or in saltation above the bed. This regime is especially important in mountain streams and is mostly responsible for the morphological evolution of rivers. The limited understanding of the physical processes involved, reflected by the poor agreement between prediction and field measurement of transport rate [1], motivates the development of alternative modeling approaches on this subject. In particular, Frey & Church [2, 3] noted the interest to analyze the phenomenon focusing on the granular phase behavior, and using the recent important developments made in the granular media community [4].

The dry $\mu(I)$ granular rheology developed in the past few years [5] has been extended to cases with interstitial fluid [6, 7, 8], and has been shown to describe well various situations from immersed granular avalanches [6, 9, 10] to sediment transport [11, 12, 13].

In the present paper, we study the rheology of the granular phase in bedload transport using a numerical model coupling a Discrete Element Method (DEM) with a 1D volume-averaged fluid momentum balance. This model has been designed to focus on the granular phase and allows to explicitly compute the particle phase stress tensor through the contact forces. The paper is organized as follows, the model is presented in section 2, and section 3 is devoted to an application to bedload transport with a special focus on the dense granular rheology.

2 Numerical model

2.1 Discrete Element Method

Discrete element method has been first applied to granular media by Cundall & Strack [14], and has recently known an important interest in the community with the increasing computational power. It consists in resolving the motion of each sphere using Newton's law, expressing the contact forces explicitly with defined contact laws depending on particles overlap. Considering bedload, the particles also undergo hydrodynamical forces so that the evolution of the position \vec{x}^p of each particle p is expressed as:

$$m \frac{d^2 \vec{x}^p}{dt^2} = \vec{f}_c^p + \vec{f}_g^p + \vec{f}_f^p, \quad (1)$$

where \vec{f}_c^p are the contact forces, \vec{f}_g^p is the gravity force and \vec{f}_f^p represents the force applied by the fluid on the particle. The latter will be detailed in section 2.3. The contact law used is the classical spring-dashpot law which defines a constant restitution coefficient and allows to describe both quasi-static and dynamical regimes encountered in bedload. The open-source DEM code Yade [15] is used.

2.2 Fluid phase resolution

The fluid phase is described using a volume-averaged description based on the averaged continuous two-phase equations [16]. Considering bedload at equilibrium, the fluid equation can be simplified using steady, unidirectional and uniform flow assumptions. Consequently the average fluid velocity reduces to its streamwise component $\langle u_x^f \rangle$ and depends only on the wall-normal direction z . The equation reads [13]:

$$0 = \frac{d \langle \tau_{xz}^f \rangle}{dz} + \frac{d R_{xz}^f}{dz} + \epsilon \rho^f g \sin \alpha - n \langle f_x \rangle^s, \quad (2)$$

where ϵ is the fluid volume fraction, ρ^f is the fluid density, $\langle \tau_{xz}^f \rangle$ is the averaged fluid viscous stress tensor, R_{xz}^f is the Reynolds stress tensor, g is the acceleration of gravity, α is the slope angle, and $n \langle f_x \rangle^s$ is the average momentum transfer associated to the fluid force transmitted to the granular phase. The operators $\langle \cdot \rangle^s$ and $\langle \cdot \rangle$ denote spatial averaging over respectively the solid and the fluid phase.

To close equation 2, the fluid is considered as newtonian so that:

$$\langle \tau_{xz}^f \rangle = \rho^f \nu^f \frac{d \langle u_x^f \rangle}{dz}, \quad (3)$$

where ν^f is the clear fluid kinematic viscosity. The average effect of the turbulent velocity fluctuations is taken into account in the Reynolds stress tensor. We adopt for simplicity a mixing length formulation, therefore R_{xz}^f reads:

$$R_{xz}^f = \rho^f \nu^t \frac{d \langle u_x^f \rangle}{dz} \quad \text{with} \quad \nu^t = \epsilon l_m^2 \left| \frac{d \langle u_x^f \rangle}{dz} \right|, \quad (4)$$

in which the mixing length l_m formulation proposed by Li & Sawamoto[17] is used:

$$l_m(z) = \kappa \int_0^z \frac{\phi^{max} - \phi(\zeta)}{\phi^{max}} d\zeta, \quad (5)$$

where $\kappa = 0.41$ represents the von Karman constant.

To finish, the term associated to the fluid-solid $n \langle f_x \rangle^s$ interaction will be detailed in the next section.

2.3 Fluid/Solid coupling

The main difficulty lies in the coupling of the two phases: discrete particle phase and continuous fluid phase. The influence of the fluid phase is represented in the solid phase model through the hydrodynamical forces \vec{f}_f^p applied on each particle in the corresponding equation of motion. In the present model, for simplification only the main hydrodynamical forces are taken into account, i.e. drag \vec{f}_D^p and buoyancy \vec{f}_b^p forces. The drag force formulation account for local particle Reynolds number (Re_p) and solid volume fraction (ϕ) dependencies, as follows:

$$\vec{f}_D^p = \frac{1}{2} \rho_f \frac{\pi d^2}{4} C_D \left\| \left\langle \vec{u}^f \right\rangle_{\vec{x}^p} - \vec{v}^p \right\| \left(\left\langle \vec{u}^f \right\rangle_{\vec{x}^p} - \vec{v}^p \right), \quad (6)$$

where $\left\langle \vec{u}^f \right\rangle_{\vec{x}^p} - \vec{v}^p$ is the relative velocity between the particle and the average fluid velocity taken at the particle center, and the drag coefficient C_D is expressed as [13, 18]:

$$C_D = \left(0.4 + \frac{24.4}{Re_p} \right) (1 - \phi)^{-3.1}. \quad (7)$$

The buoyancy force is classically applied in the wall-normal direction considering the buoyant weight of each particles.

The coupling for the fluid phase is achieved through the volume fraction $\epsilon = 1 - \phi$ and the average momentum transfer term associated with the interaction term $n \langle f_x \rangle^s$. These terms have to be evaluated at each fluid resolution step from the particles positions and applied drag forces in the streamwise direction. The expression of the average should be consistent with the one used for the derivation of the fluid momentum balance equation. We use the definition of Jackson [16] with a step weighting function of the size of the system in the streamwise and spanwise directions. The wall-normal length scale is limited by the strong mean fields gradients in this direction. Therefore, the streamwise and spanwise sizes of the system has to be taken such that statistical convergence of the averaged quantities is ensured.

The model was compared satisfactorily to existing particle-scale experiments [19], and showed to be robust with respect to the numerical parameters [20].

3 Dense granular flow rheology in bed load transport

In the dense granular flow regime, the $\mu(I)$ rheology is a consistent constitutive law for the shear and normal stresses [4, 5]. The dimensional analysis shows that the particle shear (τ_{xz}^p) to normal ($P^p = \tau_{zz}^p$) stress ratio μ is a function of a single dimensionless number $I = \frac{\dot{\gamma} d}{\sqrt{P^p / \rho^p}}$, where $\dot{\gamma}$ is the shear rate. This dimensionless number can be viewed as the ratio between a macroscopic timescale $t_{macro} = 1/\dot{\gamma}$, and a local re-arrangement timescale $t_{ff} = \frac{d}{\sqrt{P^p / \rho^p}}$. The latter corresponds to the time needed for a particle to settle over a distance d under a confining granular pressure P^p . With these definitions, the

Table 1: Definition and characteristic values of the main dimensionless numbers associated with the problem, where d the particles diameter, u_* the shear velocity, and \bar{u}^f the average fluid velocity in water depth h .

θ	Re_p	Fr	ρ^p/ρ^f	St
$\frac{\rho^f u_*^2}{(\rho^p - \rho^f)g \cos \alpha d}$	$\frac{d \ \langle u^f \rangle - \langle v^p \rangle\ }{\nu^f}$	$\frac{\bar{u}^f}{\sqrt{gh}}$	-	$\frac{d\sqrt{\rho^p P^p}}{\eta^f}$
0.25-0.5	10^3	$\gtrsim 1$	2.5	$10^2 - 10^3$

stress ratio or friction coefficient has been shown to follow a law of the type:

$$\frac{\tau_{xz}^p}{P^p} = \mu(I) = \mu_1 + \frac{\mu_2 - \mu_1}{I_0/I + 1}, \quad (8)$$

where μ_1 , μ_2 , and I_0 are phenomenological constants. Similarly, the solid volume fraction is a unique function of I that can be described by the following formulation:

$$\phi = \phi(I) = \frac{\phi_{max}}{1 + aI}, \quad (9)$$

where ϕ_{max} is the maximum solid volume fraction.

The analysis has been generalized to dense granular flow with non-negligible interstitial fluid effects [6, 7, 8], by modifying the re-arrangement timescale according to the fluid flow regime at the particle scale: viscous or inertial. Three regimes have been identified depending on the ratio between the re-arrangement timescales associated to respectively viscous (t_{visc}), turbulent (t_{turb}), and free-fall regime (t_{ff}). The different regimes can be defined using the two dimensionless numbers $St = t_{visc}/t_{ff}$, and $r = t_{turb}/t_{ff}$. For $St \gg 1$ and $r \gg 1$ the system is in the free-fall regime corresponding to dry granular flows for which the influence of the interstitial fluid is negligible. The viscous ($St \ll 1$ and $r \ll 1$) and turbulent regimes ($St \gg 1$ and $r \ll 1$) correspond to re-arrangement timescales dominated respectively by the viscous and turbulent drag contribution. For the viscous and free-fall regimes, the dense granular flow has been shown to follow a $\mu(I)/\phi(I)$ rheology. The dimensionless number being different for the different regimes [6, 7, 8, 9, 10, 13, 21]. The authors are aware of a single contribution on the turbulent regime [21].

Applying the volume averaging operator to the particle stress tensor allows to compute from DEM the average particle phase tensor for each slice of volume V $\langle \sigma_{ij}^p \rangle$ [4, 22]:

$$\langle \sigma_{ij}^p \rangle = -P^p \delta_{ij} + \tau_{ij}^p = -\frac{1}{V} \sum_{\alpha \in V} m^\alpha v_i'^\alpha v_j'^\alpha - \frac{1}{V} \sum_{c \in V} f_i^c b_j^c, \quad (10)$$

where the sum are respectively over the particles and the contacts contained in the volume V , $v_k'^\alpha = v_k^\alpha - \langle v_k \rangle$ is the k component of the spatial velocity fluctuation associated with particle α of mass m^α , f^c the contact force applied by particle 1 on particle 2, and b^c the branch vector from particle 1 to particle 2.

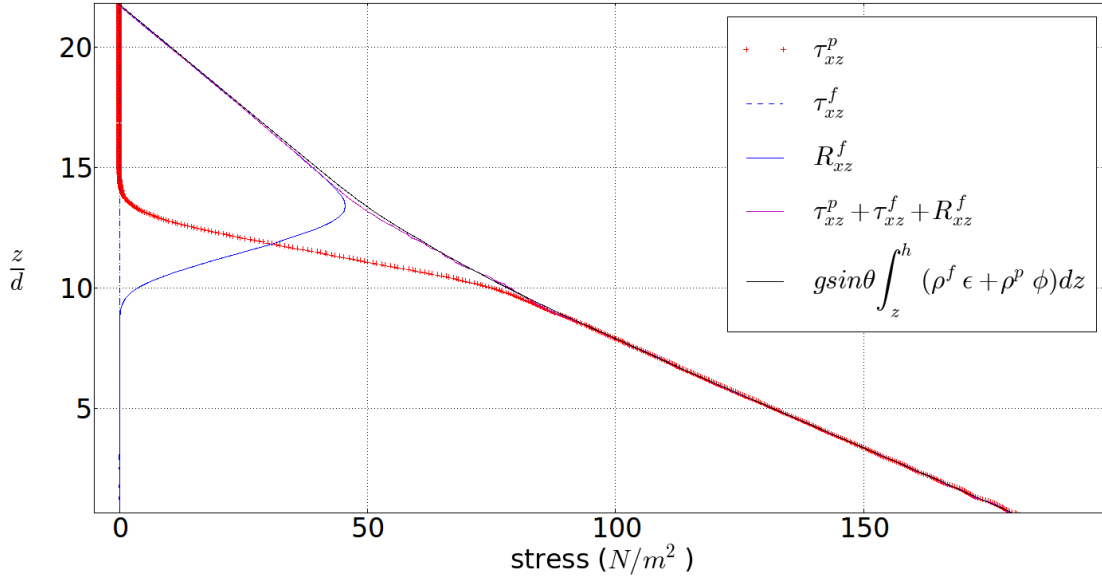


Figure 1: Momentum balance of the mixture as a function of the depth for the case $\theta \sim 0.5$.

Two bed load simulations have been carried out corresponding to rather intense sediment transport. The turbulent fluid flow is driven by gravity, the slope is fixed to 0.1, and the water depth is varied to modify the fluid bed shear stress imposed on the granular bed τ_b^f . The dimensionless number describing bed load is called the Shields number $\theta = \tau_b^f / \Delta \rho g d$ and corresponds to the ratio of the force exerted by the fluid on the granular bed to the buoyant weight of a single particle. The two bedload configurations considered here corresponds to Shields numbers of $\theta \sim 0.25$ and $\theta \sim 0.5$. Table 1 presents the different characteristic dimensionless numbers associated with these two cases. Mono-disperse spherical beads are considered and periodic boundary conditions are used for the granular phase in the streamwise and spanwise directions. The domain size is taken as $l_x = l_y = 30 d$, with 10 layers of grains. To resolve accurately the wall-normal gradients, l_z is taken as $d/30$ [20]. For each simulation, the particles are deposited under gravity and the fluid flow profile is resolved approximately every 100 DEM timesteps with no-slip boundary condition at the bottom and imposed free-surface position. After reaching equilibrium, results are averaged over 100 seconds and the different averaged variables are obtained for each layer as a function of the depth.

From the knowledge of the particle and fluid stress tensor profiles, it is possible to back compute the mixture momentum balance profile. With unidirectional, uniform and steady assumptions, the streamwise component of the average momentum balance of the mixture reads:

$$0 = \frac{d\tau_{xz}^f}{dz} + \frac{dR_{xz}^f}{dz} + \frac{d\tau_{xz}^p}{dz} + g \sin \alpha (\rho^p \phi + \rho^f \epsilon) \quad (11)$$

Integrating between z and the surface h leads to:

$$0 = -\tau^f(z) - R_{xz}^f(z) - \tau_{xz}^p(z) + g \sin \alpha \int_z^h (\rho^p \phi + \rho^f \epsilon) dz. \quad (12)$$

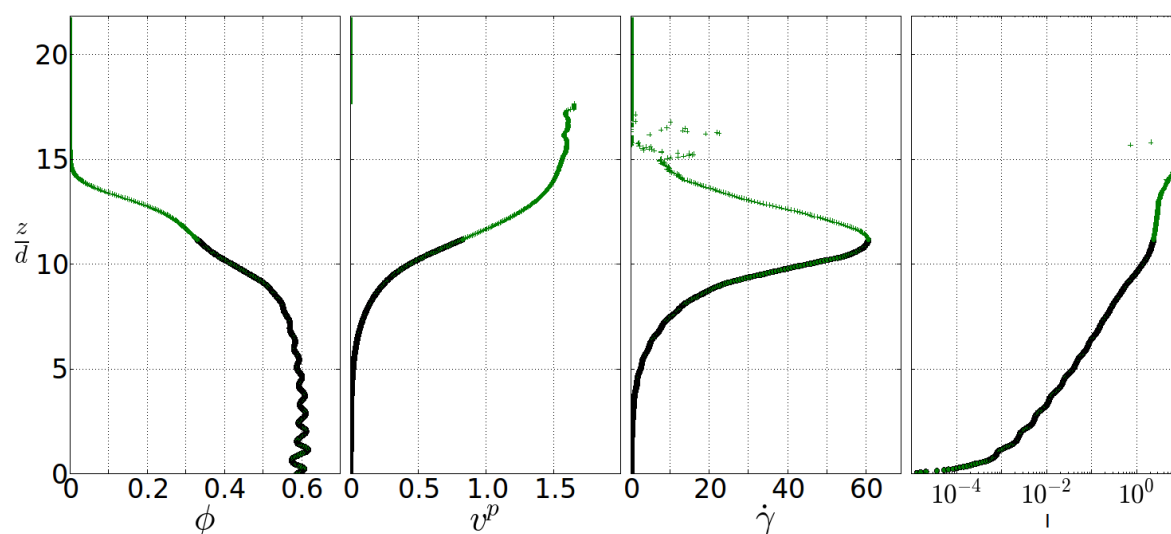


Figure 2: Average depth profiles of solid volume fraction ϕ , particle velocity v^p and shear rate $\dot{\gamma}$, and inertial number I , for the case $\theta \sim 0.5$.

This gives valuable informations on the mechanisms at work for the different vertical positions in the flow. Figure 1 shows the vertical profile of the mixture momentum balance and the different contributions for case $\theta \sim 0.5$. The first important comment is that the momentum balance is closed, i.e. the particle and fluid shear stress tensors equilibrate the gravity contribution. This is consistent with the steady flow assumption and it also suggests that the particle stress tensor profile is accurately evaluated. Regarding the different profiles, the lower part is dominated by the particle shear stress, while the upper part is dominated by the turbulent one. In the middle part a competition between these two contributions takes place. The viscous stress tensor appears to be negligible at all vertical positions in agreement with the high value of the Reynolds number.

Figure 2 presents average depth profiles of solid volume fraction ϕ , particle velocity v^p , shear rate $\dot{\gamma}$ and inertial number I , using the fluid mechanics convention. We recover the decomposition in two parts observed in the momentum balance. The particle shear rate shows a clear transition with a peak at the interface. Based on the position of this peak, the results are highlighted with two different symbols: \bullet in the grain-dominated part, and $+$ in the fluid-dominated one. The solid volume fraction profile ϕ shows a typical variation from the random loose packing fraction inside the fixed bed to zero above the bed. The decreasing trend is marked by the presence of a concentration shoulder. The velocity profile follows an exponential increase at the transition from the fixed, quasi-static, bed with an inflexion point around the concentration shoulder. Above, the fluid flow exhibits a logarithmic profile (not shown here) characteristic of a turbulent boundary layer. In the right panel, the inertial number profile is presented in log scale, the values ranges from very low value in the lower part, corresponding to a quasi-static regime, to order 10 in the upper part, corresponding to very inertial regime. The $\mu(I)$ rheology is expected to apply for inertial number values lower or equal to unity at most.

Figure 3 presents the particle shear to normal stress ratio and solid volume fraction versus the inertial number for two the bedload simulations ($\theta \sim 0.5$ and $\theta \sim 0.25$). The points corresponding to the lower part, represented by \bullet , nicely collapse on a single curve that can be fitted by a $\mu(I)/\phi(I)$ (8,9) law. A best fit gives the following phenomenological constants $\mu_1 = 0.35$, $\mu_2 = 0.97$, $I_0 = 0.69$, $\phi_m = 0.6$

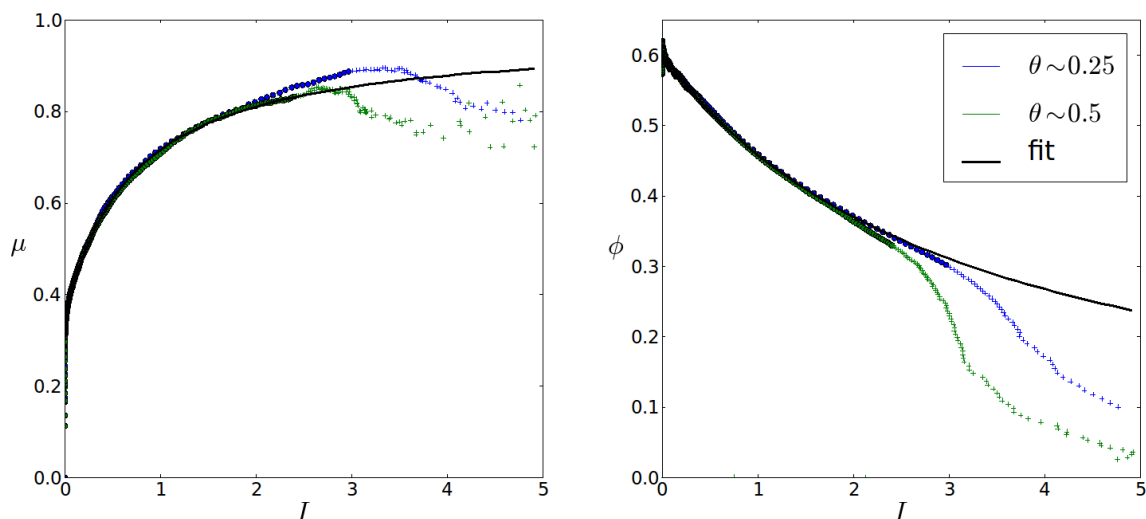


Figure 3: The particle shear to normal stress ratio μ and the solid volume fraction ϕ are plotted as functions of the inertial number. The two parts shows different behavior with a clear trend in the dense flow, and a more chaotic one in the fluid-dominated part. The dense part can be fitted by a law of type $\mu(I)/\phi(I)$ (8,9) with phenomenological constants $\mu_1 = 0.35$, $\mu_2 = 0.97$, $I_0 = 0.69$, $\phi_m = 0.6$ and $a = 0.31$ (fit).

and $a = 0.31$. These values are slightly different from those obtained for dry granular flows. The collapse observed as a function of the inertial number confirms that the bedload cases considered here are in the free-fall regime. In the fluid-dominated layer, the results do not collapse versus the inertial number and other mechanisms than contacts/collisional interactions come into play. Future work will focus on this point.

4 Conclusion

The results presented herein shows that the proposed methodology allows to study the local granular rheology in bed load transport from numerical simulations. The main conclusion is that a $\mu(I)/\phi(I)$ rheology allows to describe the granular rheology in bed-load transport for two different Shields numbers at least in the denser part of the granular flow. In the upper part, the inertial number alone can not represent the simulations and further work has to be done to determine if it is dominated by binary collisional interactions (kinetic theory) or driven by the fluid flow. The present results will be extended in a near future to investigate the influence of the particle properties: density and diameter.

Acknowledgements

This research was supported by Irstea (formerly Cemagref), the French Institut National des Sciences de l'Univers programme EC2CO-BIOHEFECT, and the french national program EC2CO-LEFE « MODSED ».

References

- [1] J. Bathurst. Effect of coarse surface layer on bed-load transport. *Journal of Hydraulic Engineering*, 133(11):1192–1205, 2007.
- [2] P. Frey and M. Church. How river beds move. *Science*, 325:1509–1510, 2009.
- [3] P. Frey and M. Church. Bedload : a granular phenomenon. *Earth Surface Processes and Landform*, 36:58–69, 2010.
- [4] B. Andreotti, Y. Forterre, and O. Pouliquen. *Granular media: between fluid and solid*. Cambridge University Press, 2013.
- [5] GDR Midi. On dense granular flows. *The European Physical Journal E*, 14(4):341–365, 2004.
- [6] S. Courrech du Pont, P. Gondret, B. Perrin, and M. Rabaud. Granular avalanches in fluids. *Phys. Rev. Lett.*, 90:044301, Jan 2003.
- [7] C. Cassar, M. Nicolas, and O. Pouliquen. Submarine granular flows down inclined planes. *Physics of Fluids (1994-present)*, 17(10):–, 2005.
- [8] F. Boyer, É. Guazzelli, and O. Pouliquen. Unifying suspension and granular rheology. *Phys. Rev. Lett.*, 107:188301, Oct 2011.
- [9] D. Doppler, P. Gondret, T. Loiseleux, S. Meyer, and M. Rabaud. Relaxation dynamics of water-immersed granular avalanches. *Journal of Fluid Mechanics*, 577:161–181, 4 2007.
- [10] M. Pailha and O. Pouliquen. A two-phase flow description of the initiation of underwater granular avalanches. *Journal of Fluid Mechanics*, 633:115–135, 8 2009.
- [11] M. Ouriemi, P. Aussillous, and E. Guazzelli. Sediment dynamics. part 1. bed-load transport by laminar shearing flows. *Journal of Fluid Mechanics*, 636:295–319, 10 2009.
- [12] P. Aussillous, J. Chauchat, M.I Pailha, M. Médale, and E. Guazzelli. Investigation of the mobile granular layer in bedload transport by laminar shearing flows. *Journal of Fluid Mechanics*, 736:594–615, 12 2013.
- [13] T. Revil-Baudard and J. Chauchat. A two-phase model for sheet flow regime based on dense granular flow rheology. *Journal of Geophysical Research: Oceans*, 118(2):619–634, 2013.
- [14] P. A. Cundall and O. D. L. Strack. A discrete numerical model for granular assemblies. *Géotechnique*, pages 305–329(24), 1979.
- [15] V. Šmilauer, E. Catalano, B. Chareyre, S. Dorofeenko, J. Duriez, A. Gladky, J. Kozicki, C. Modenese, L. Scholtès, L. Sibille, J. Stránský, and K. Thoeni. *Yade Documentation (V. Šmilauer, ed.)*, *The Yade Project, 1st ed.*, <http://yade-dem.org/doc/>, 2010.
- [16] R. Jackson. *The dynamics of fluidized particles*. Cambridge University Press, 2000.
- [17] L. Li and M. Sawamoto. Multi-phase model on sediment transport in sheet-flow regime under oscillatory flow. *Coastal engineering Japan*, 38:157–178, 1995.

-
- [18] J.T. Jenkins and D.M. Hanes. Collisional sheet flows of sediment driven by a turbulent fluid. *Journal of Fluid Mechanics*, 370:29–52, 1998.
- [19] P. Frey. Particle velocity and concentration profiles in bedload experiments on a steep slope. *Earth Surface Processes and Landforms*, 39(5):646–655, 2014.
- [20] R. Maurin, J. Chauchat, B. Chareyre, and P. Frey. A minimal coupled dem-fluid phase model for bedload transport. *submitted to Physics of Fluids*.
- [21] E. Izard, T. Bonometti, and L. Lacaze. Simulation of an avalanche in a fluid with a soft-sphere/immersed boundary method including a lubrication force. *The Journal of Computational Multiphase Flows*, 6(4):391–406, 2014.
- [22] I. Goldhirsch. Stress, stress asymmetry and couple stress: from discrete particles to continuous fields. *Granular Matter*, 12(3):239–252, 2010.